Diamond & Related Materials 126 (2022) 109058

Contents lists available at ScienceDirect

Diamond & Related Materials

journal homepage: www.elsevier.com/locate/diamond

Cleaning diamond surfaces via oxygen plasma inhibits the formation of a TiC interface

Holly M. Johnson [a], Jesse M. Brown [a,b], Anna M. Zaniewski [a,b], Robert J. Nemanich [a,*]

[a] Arizona State University Department of Physics, Tempe, AZ 85287-1504, United States of America
[b] Advent Diamond Inc., Scottsdale, AZ 85257, United States of America

ARTICLE INFO

Keywords:
Diamond
X-ray photoelectron spectroscopy
Plasma
Surface etching
Thin film characterization
Metals

ABSTRACT

TiC at the diamond-titanium interface is known to be a stable and beneficial layer for diamond based electronic devices. However, certain cleaning steps can alter the chemical composition of this interface. One such process is oxygen plasma etching, which terminates the surface of the diamond with oxygen. Oxygen is highly reactive with titanium, forming titanium oxides. Theoretically the titanium-diamond interface can be improved through sufficient annealing after device fabrication. To test this, we investigated the interface of oxygen-terminated polycrystalline B-doped diamond and titanium via XPS in an effort to determine if oxygen would rearrange away from the diamond surface and TiC would be formed through post-deposition annealing. After annealing at temperatures up to 900 °C, it was found that TiC was not detected at any point in this experiment. Oxygen-termination, despite its de-scumming capabilities, likely inhibits the formation of TiC at the diamond surface.

1. Introduction

There is currently a renaissance of interest in diamond as a semiconductor. Proposed and realized solid-state diamond devices include a wide range of applications, from quantum information processing [1] to radiation detection [2–4], to photochemistry [5], and power management [6,7]. These applications are made possible by diamond's remarkable physical properties, which include the largest thermal conductivity of any natural material [8], extreme figures of merit for power handling applications [9], large electron and hole mobilities [8], large bandgap, and the ability to manipulate point defects of N—V centers to probe electron spin [10,11].

For electronics, one particularly salient property of diamond is that its surface termination has a large impact on the surface energy, enabling tuning across an electron affinity energy range spanning approximately 4.5 eV [5,12,13]. For many applications, metal contacts play a pivotal role in performance, with surface termination, such as with hydrogen or oxygen, playing a significant role in whether a given metal will result in the formation of Schottky or Ohmic type contacts [14]. Prior literature has particularly revealed that the formation of titanium-carbide is a stable and beneficial layer for diamond electronics [15,16]. Despite this well-established observation, many diamond electronics device fabrication steps continue to rely upon oxygen plasma as a cleaning step without a clear understanding of how this processing step impacts the formation of the titanium-carbide layer. TiC is a useful layer for diamond-based devices as it creates a strong contact between the metal overlayers and the diamond surface [17]. A TiC interface will also facilitate the transfer of heat as it has a high thermal conductivity [17,18]. Most notably, TiC at the interface has been observed in correlation with high-performing Ohmic contacts to diamond [16].

Hence, an investigation into how O-termination of the sample surface affects the formation of TiC will further understanding of the diamond-metal interface.

Therefore, in this study, we are interested in how this oxygen plasma cleaning process enables or inhibits the formation of titanium carbide, and we intentionally leave the oxygen termination on the diamond surface after using an oxygen plasma de-scumming recipe. We iteratively anneal the diamond and use X-ray photoemission spectroscopy (XPS) to study the evolution of the surface chemical properties, as shown in Fig. 1. We find that the standard de-scumming oxygen plasma recipe is detrimental to the formation of titanium carbide. In fact, despite annealing the sample up to 900 °C, titanium carbide was not detected. We do find evidence of titanium oxide with evolving stochiometry, raising the question of rearrangement of oxygen. Polycrystalline boron-doped diamond was chosen for this study since this material is available for devices which require large-area substrates.

* Corresponding author.
E-mail address: robert.nemanich@asu.edu (R.J. Nemanich).

https://doi.org/10.1016/j.diamond.2022.109058
Received 7 October 2021; Received in revised form 26 March 2022; Accepted 18 April 2022
Available online 21 April 2022

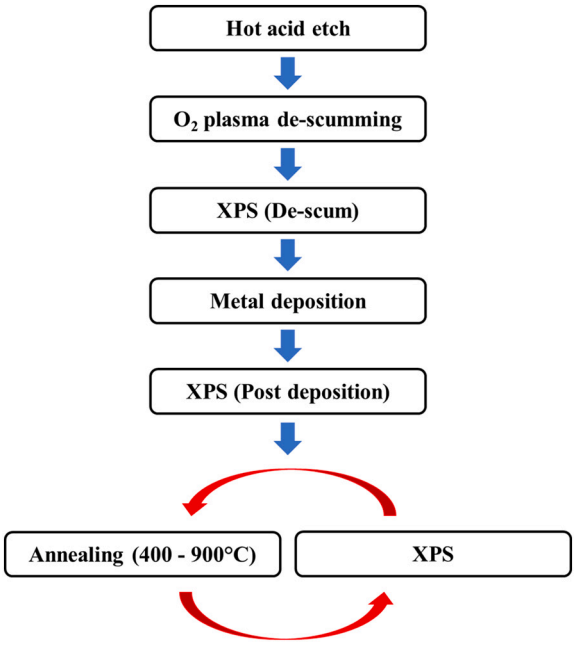

Fig. 1. Experimental flowchart depicting the cleaning, fabrication, and data collection steps. Following an initial XPS analysis of the sample, the sample is iteratively annealed in steps of 100 °C from 400 °C to 900 °C, taking XPS after each annealing temperature.

2. Methods

The boron-doped polycrystalline diamond used in this experiment (dimensions 5 × 5 mm, 0.45 mm; resistivity $2 \cdot 10^{-3}$ Ω·cm; doping concentration [B] = $2 \cdot 10^{20}$-$6 \cdot 10^{20}$; supplied by Element Six) has a rough side (Ra ~ 50 μm) and smooth side (Ra < 30 nm). Metal is deposited onto the smooth side of the substrate.

The diamond is first cleaned via a hot acid etch, which is a standard technique for removing organic contaminants. The specific recipe used is 20 mL of sulfuric acid (H_2SO_4) and 5 mL of nitric acid (HNO_3), at a temperature of 220 °C for 20 min. The sample is then allowed to cool in the acid bath for an additional 20 min. Following this treatment, the sample is washed in deionized water and dried using compressed nitrogen gas.

After the acid cleaning, the sample is cleaned again using plasma, specifically, reactive ion etching. This process is, in fact, the same process used to etch diamond [19], which cleans the surface through the removal (and inherent damaging) of monolayers at the diamond's surface [20]. The plasma is primarily oxygen-based, with a 50:2 O:SF_6 ratio. The plasma is held at a power of 200 W and the sample is etched for 10 s. This process will be referred to as the plasma de-scumming. De-scumming is used to remove any contamination, for instance, from photolithography, and also has the effect of O-terminating the surface of the diamond, which provides improved adhesion.

The sample is then transferred to an electron beam evaporator (Kurt J. Lesker PVD75 PROLine) to deposit layers of titanium (20Å) and platinum (10Å). For each deposition, the chamber is maintained at a pressure of $5 \cdot 10^{-6}$ Torr and the metals are deposited at a rate of 1.00 ± 0.10Å/s. The platinum was deposited in an effort to slow the oxidation process of titanium, which occurs rapidly in atmosphere. Although device design often also includes a layer of gold, we did not include this layer in order to maintain transparency for XPS.

Following the cleaning steps and metal deposition, the sample is mounted on a nichrome (Ni/Cr/Nb) plate with tantalum wires, bound to a molybdenum sample holder, and quickly loaded into the load lock of an integrated vacuum system, with a base pressure $5 \cdot 10^{-9}$ Torr, allowing the sample to be transferred *in-situ* between annealing chamber (base pressure $3 \cdot 10^{-9}$ Torr) and XPS chamber (base pressure $5 \cdot 10^{-10}$ Torr).

The X-ray source is a monochromatic Al-Kα X-ray with an energy centered around 1486.6 eV with a bandwidth of 0.2 eV and a 7 × 2 mm spot size that is aligned with the diagonal of the 5 × 5 mm diamond to maximize the sample signal. The hemispherical analyzer has a slit size of 0.4 mm. A pass energy of 100 eV gives an energy resolution of 150 meV. The energy resolution of the spectrometer and X-ray source makes a base FWHM of all the photoelectron peaks to be approximately 0.35 eV. A four-element electrostatic lens is used in sweep mode to scan the range of photoelectron energies excited by the X-ray source.

The wide energy range XPS analysis of the sample, shown in Fig. 2, reveals that following the descumming process the diamond surface is oxygen terminated, with no other peaks or contamination detected. This oxygen termination is also seen in the C1s XPS data following descumming as a small shoulder near 288 eV in Fig. 3a. This binding energy likely arises from carbon-oxygen bonding at the diamond surface.

Following the initial metal deposition step, the wide energy range XPS spectrum shows the presence of oxygen, titanium, platinum, and carbon, as expected.

In the UHV annealing chamber, the sample is radiatively heated by a toroidal tungsten coil at a pressure on the order of 10^{-8} Torr and monitored with a Mikron M90Q optical pyrometer. The annealing process was iterative, increasing the temperature from 400 °C to 900 °C in increments of 100 °C. Temperatures are maintained for 25 min with a ramp rate of 25 °C/min ± 5 °C/min. XPS measurements were taken after de-scumming, after metal deposition, and between each annealing step.

3. Results

The XPS data of the C1s and Ti 2p core levels are shown in Fig. 3a and b, respectively. This collected data revealed several peaks; in order to determine the total XPS profile, the individual peaks were fit using a series of Gaussian peaks, shown as the grey curves, and these peaks are combined to recreate the total observed profile, shown in orange. Only peaks with binding energies less than 466 eV were used in this fit, and the data outside of this region is considered background.

Analysis of this data showed that titanium carbide was not observed

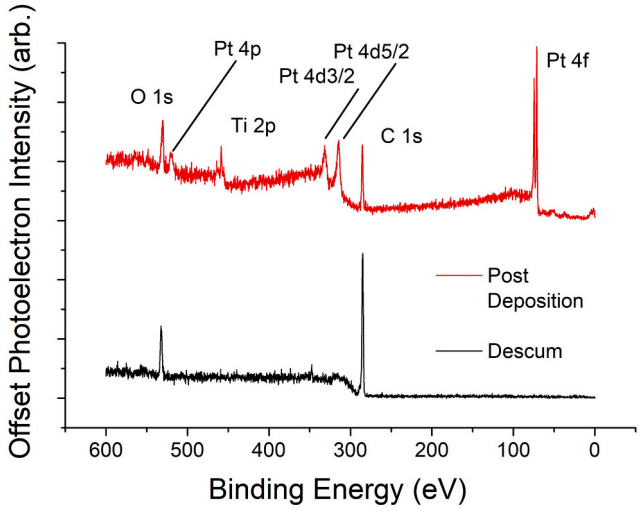

Fig. 2. XPS data of the diamond sample after de-scumming and immediately post-deposition. There is clear oxidation on the sample surface before deposition takes place, along with a strong carbon peak depicting the diamond; there are no signs of other elements or contamination. Post-deposition and pre-annealing, there are peaks showing the Ti and Pt overlayer as well as oxygen. TiC features were not detected post-deposition. To contrast with a sample that was intentionally fabricated without an oxygenated surface and which does show TiC at the diamond interface, refer to [16].

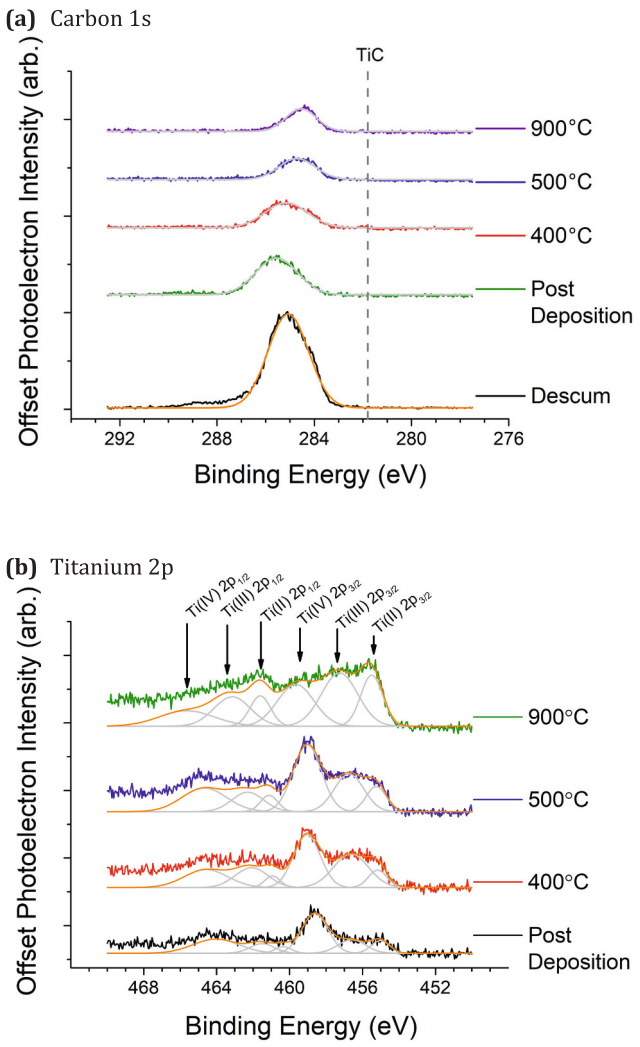

Fig. 3. (a) C1s XPS data of the diamond sample at different steps in the experiment. Post de-scumming, the peak is consistent with B-doped polycrystalline diamond. The intensity of this peak diminishes post-deposition due to the Ti/Pt overlayer. *Note*: The dotted line on this figure represents the expected value of C1s binding energy for TiC (281.8 eV). (b) Ti 2p XPS data of the diamond-titanium interface including the data taken post deposition and after annealing at 400, 500, and 900 °C. Peaks are fit to titanium oxidation states as labeled. The lack of the TiC peak in the C1s data indicates that the peak near 455 eV in the Ti 2p spectrum originates from the Ti (II) 2p oxidation state and not the titanium-carbon bond.

at any annealing temperature. Data supporting this conclusion can be found in Fig. 3a and b, which shows the C1s and Ti 2p XPS spectra at various points in this experimental process (Fig. 1). Fig. 3a directly indicates the binding energy of TiC in the C1s spectrum with a vertical, dotted line, where a peak would be present at this binding energy if TiC were detectable. The lack of signal for TiC is clear in these spectra, as there is extremely little to no signal at the C1s binding energy of TiC (281.8 eV). In contrast, similar boron-doped polycrystalline samples which had the oxygen intentionally removed and were subsequently topped with titanium are known to show TiC at this position [16].

The data shown in Fig. 3b has peaks consistent with TiO_2 $2p_{1/2}$ (464.70 eV), Ti_2O_3 $2p_{1/2}$ (462.0 eV), TiO_2 $2p_{3/2}$ (458.70 eV), and TiO $2p_{3/2}$ (455.90 eV). These peaks are further analyzed to better understand how the oxidation states of the titanium layer evolve following each annealing step. The results of this analysis are shown in Fig. 4 and Table I.

In Fig. 4, to determine the percentage of each titanium oxidation state present in the scan, we calculate the ratio of each oxidation state peak intensity from both the $2p_{1/2}$ and $2p_{3/2}$ energies and compare to the total Ti 2p peak area. For example, for TiO, we calculate the ratio of the peak area from the TiO $2p_{1/2}$ and TiO $2p_{3/2}$ energies to the total Ti 2p area to find its percentage after each step. The other oxidation state percentages are similarly defined and plotted in Fig. 4.

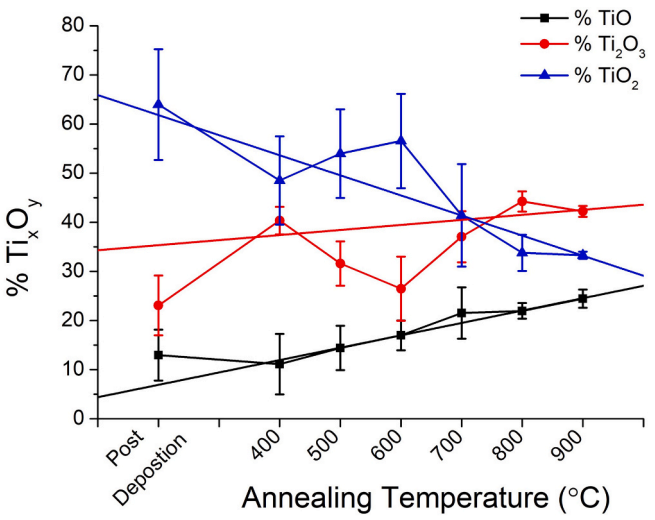

Fig. 4. Percent of titanium oxide which is composed of TiO, Ti_2O_3, and TiO_2 as determined by extrapolation from Fig. 3 XPS data. As the sample is annealed at higher temperatures, the TiO_2 decreases while the TiO increases.

Table I
Oxygen to titanium ratio observed by XPS.

Process step	Temperature [°C]	Stoichiometry [O:Ti]
De-scum	–	–
Metal deposition	–	2.21
1st heating	400	1.52
2nd heating	500	1.49
3rd heating	600	1.50
4th heating	700	1.28
5th heating	800	1.20
6th heating	900	1.18

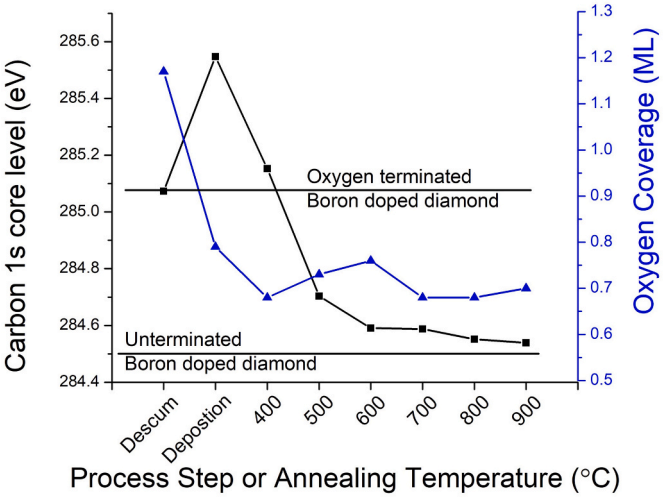

Fig. 5. The boron-doped diamond *C* 1s core level energy peak center shift (black) is shown and compared to the calculated oxygen monolayer coverage (blue). (For interpretation of the references to color in this figure legend, the reader is referred to the web version of this article.)

Shown in Fig. 5 are the oxygen coverage in monolayers (ML) as analyzed by the C1s and O 1s peak areas, and the C1s core level peak position. The initial boron doped oxygen terminated diamond surface core level energy (285.2 eV) is consistent with other previous reports [21]. The calculated oxygen coverage after the de-scum is approximately 1.2 ML, which is expected. After metal deposition, the C1s core level energy is shifted to higher binding energy (285.6 eV) while the oxygen coverage drops to approximately 0.79 ML. The C1s peak center is about 1.1 eV greater after titanium metal deposition than for a clean boron-doped diamond surface (284.5 eV). After annealing to 400 °C, the core level returns to the initial oxygen terminated binding energy (285.1 eV), however, the oxygen coverage reduces to about 0.63 ML. After annealing to 500 °C, the oxygen coverage increases slightly to 0.73 ML and the C1s core level shifts to 284.7 eV. This is approaching the "unterminated boron-doped diamond" energy level (284.5 eV) [21]. The C1s binding energy then remains relatively constant but continues to trend toward 284.5 eV with increasing annealing temperature. The oxygen monolayer coverage trends to 0.70 ML at 700 °C and above. No changes in color or appearance were observed.

Oxygen to titanium ratios (O:Ti) are calculated using the total peak area for each element divided by the atomic sensitivity factor, which for oxygen and titanium is 0.66 and 1.8 respectively [22].

$$O:Ti = \frac{A(O)}{0.66} * \frac{1.8}{A(Ti)}$$

where *A(O)* is the total peak area of oxygen and *A(Ti)* is the total peak area of titanium. These ratios are compiled and shown in Table I.

4. Discussion

Reviewing the XPS data taken throughout this experiment shows that TiC was not detected in this experiment. In contrast, samples prepared with a de-oxygenated surface are known to have the TiC peak present at 281.8 eV [16,23]. Since TiC could not be observed via XPS, it can be reasoned that TiC was not significantly present in our samples, unable to form at the diamond-titanium interface even after annealing at temperatures up to 900 °C. This is a remarkable result, as TiC is the most common Ohmic contact on diamond and is routinely fabricated through the deposition and annealing of titanium on the diamond surface [24,25].

At first glance, the lack of TiC formation might suggest that the oxygen terminated diamond interface is unchanged by annealing to these temperatures. However, the shift in the carbon core level C1s, from 285.0 eV after de-scum to 284.5 eV after annealing to temperatures ≥500 °C, and the changes in the oxygen coverage (Fig. 5) shows that the carbon oxygen interface has changed. This carbon peak shift to lower binding energies is consistent with a reduction of oxygen at the diamond surface [26].

The titanium spectra show the titanium oxidation states reducing, the Ti_XO_Y concentration shifting from TiO_2 to Ti_2O_3, as seen in Fig. 4. The shift in carbon core level, reduction of the titanium oxidation states, and lack of sufficient pure titanium (at 454.0 eV) to uptake additional oxygen into TiO_X formations, suggests that oxygen is being redistributed during the annealing process.

The carbon peak area also decreases after annealing at 400 °C and further decreases at 500 °C, but is constant from 500 °C and above. This has a few possible explanations: one is that more material is being deposited on the surface, which is highly unlikely, or that there is a change in the inelastic mean free path (IMFP) of the *C* 1s photoelectrons from 3.2 nm to 1.8 nm. The IMFP of the different oxidation states of titanium are approximately 2.4 nm, while that of platinum is approximately 1.3 nm. Another possible explanation may be related to morphological variations of the metal overlayer during the annealing process.

This result provides experimental evidence that it is possible for oxygen to be displaced and desorbed through the metal layers via post-deposition annealing. This is consistent with observations of oxygenation of metals described by [27]. Significantly, even though the oxygen appears to be redistributing, the formation of titanium carbide at the diamond interface does not automatically follow. However, if the trend of displacement of oxygen continues, longer annealing times may produce different results, and are of interest for future study.

For additional future research, X-ray diffraction (XRD) would be useful because it can directly characterize the diffusion of oxygen through the metal overlayer. This would provide further evidence to support our conclusion that the use of oxygen plasma de-scumming inhibits the formation of TiC. The effect of crystal orientation at the substrate surface on TiC formation cannot be determined from this study on polycrystalline diamond, but is also of future interest.

5. Conclusion

A diamond sample was treated with a commonly used fabrication step, an oxygen plasma-based de-scumming process, and the evolution of the interface between the diamond and a subsequently deposited titanium overlayer was studied. The results show that titanium which comes into contact with O-terminated diamond forms various titanium-oxide bonds. Upon annealing, oxygen redistributes and oxygen bonds rearrange to form increasingly reduced forms of Ti_XO_Y, but the diamond-titanium interface does not sufficiently rearrange to form TiC.

CRediT authorship contribution statement

Holly M. Johnson and Jesse M. Brown established the methodology, performed the experiments, analyzed the data, and contributed to the manuscript preparation. Anna M. Zaniewski and Robert J. Nemanich conceptualized the project and contributed to the manuscript preparation.

Declaration of competing interest

The authors declare that they have no known competing financial interests or personal relationships that could have appeared to influence the work reported in this paper.

Acknowledgements

This work is supported through the National Science Foundation under Grant DMR-2003567.

References

[1] J. Wrachtrup, F. Jelezko, Processing quantum information in diamond, J. Phys. Condens. Matter 18 (2006) S807.
[2] A. Mainwood, Recent developments of diamond detectors for particles and uv radiation, Semicond. Sci. Technol. 15 (2000) R55.
[3] J. Holmes, M. Dutta, F.A. Koeck, M. Benipal, J. Brown, B. Fox, R. Hathwar, H. Johnson, M. Malakoutian, M. Saremi, A. Zaniewski, A 4.5 μm pin diamond diode for detecting slow neutrons, Nucl. Instrum. Methods Phys. Res., Sect. A 903 (2018) 297.
[4] J.M. Holmes, M. Dutta, F.A. Koeck, M.K. Benipal, R. Hathwar, J. Brown, B. Fox, H. Johnson, A. Zaniewski, R. Alarcon, S. Chowdhury, S.M. Goodnick, R. J. Nemanich, Neutralizing the polarization effect of diamond diode detectors using periodic forward bias pulses, Diam. Relat. Mater. 94 (2019) 162.
[5] J. Barkl, A.M. Zaniewski, F. Koeck, R.J. Nemanich, Diamond photochemistry with visible light, Diam. Relat. Mater. 96 (2019) 195.
[6] S. Shikata, Single crystal diamond wafers for high power electronics, Diam. Relat. Mater. 65 (2016) 168.
[7] M.K. Benipal, J. Brown, F. Koeck, A. Zaniewski, M.F. Ahmad, R. Nemanich, Commercialization of diamond semiconductor devices, in: 2021 IEEE Energy Conversion Congress and Exposition (ECCE), 2021, pp. 5585–5589.
[8] S. Koizumi, H. Umezawa, J. Pernot, M. Suzuki, Power Electronics Device Applications of Diamond Semiconductors, in: Woodhead Publishing Series in Electronic and Optical Materials, Elsevier Science, 2018.
[9] K. Shenai, R.S. Scott, B.J. Baliga, Optimum semiconductors for high-power electronics, IEEE Trans. Electron Devices 36 (1989) 1811.

[10] S. Prawer, I. Aharonovich, Quantum Information Processing with Diamond: Principles and Applications, in: Woodhead Publishing Series in Electronic and Optical Materials, Elsevier Science, 2014.
[11] D. Lee, K.W. Lee, J.V. Cady, P. Ovartchaiyapong, A.C.B. Jayich, Topical review: spins and mechanics in diamond, J. Opt. 19 (2017), 033001.
[12] K.J. Rietwyk, S. Wong, L. Cao, K. O'Donnell, L. Ley, A. Wee, C. Pakes, Work function and electron affinity of the fluorine-terminated (100) diamond surface, Appl. Phys. Lett. 102 (2013), 091604.
[13] K.M. O'Donnell, M.T. Edmonds, A. Tadich, L. Thomsen, A. Stacey, A. Schenk, C. I. Pakes, L. Ley, Extremely high negative electron affinity of diamond via magnesium adsorption, Phys. Rev. B 92 (2015), 035303.
[14] J. Van der Weide, R. Nemanich, Schottky barrier height and negative electron affinity of titanium on (111) diamond, J. Vac. Sci. Technol., B: Microelectron. Nanometer Struct.–Process., Meas., Phenom. 10 (1992) 1940.
[15] T. Tachibana, J. Glass, D. Thompson, Titanium carbide rectifying contacts on boron-doped polycrystalline diamond, Diam. Relat. Mater. 2 (1993) 37.
[16] T. Tachibana, B. Williams, J. Glass, Correlation of the electrical properties of metal contacts on diamond films with the chemical nature of the metal-diamond interface. ii. Titanium contacts: a carbide-forming metal, Phys. Rev. B 45 (1992) 11975.
[17] M. Sawczak, M. Sobaszek, K. Siuzdak, J. Ryl, R. Bogdanowicz, K. Darowicki, M. Gazda, A. Cenian, Formation of highly conductive boron-doped diamond on TiO2 nanotubes composite for supercapacitor or energy storage devices, J. Electrochem. Soc. 162 (2015), A2085.
[18] L. Lei, Y. Su, L. Bolzoni, F. Yang, Evaluation on the interface characteristics, thermal conductivity, and annealing effect of a hot-forged Cu-Ti/diamond composite, J. Mater. Sci. Technol. 49 (2020) 7.
[19] J. Holmes, J. Brown, F.A. Koeck, H. Johnson, M.K. Benipal, P. Kandlakunta, A. Zaniewski, R. Alarcon, R. Cao, S.M. Goodnick, R.J. Nemanich, Performance of 5μm pin diamond diodes as thermal neutron detectors, Nucl. Instrum. Methods Phys. Res., Sect. A 961 (2020).
[20] G.S. Sandhu, W.K. Chu, Reactive ion etching of diamond, Appl. Phys. Lett. 55 (5) (1989) 437.
[21] X. Liu, X. Chen, D.J. Singh, R.A. Stern, J. Wu, S. Petitgirard, C.R. Bina, S. D. Jacobsen, Boron–oxygen complex yields n-type surface layer in semiconducting diamond, Proc. Natl. Acad. Sci. 116 (2019) 7703.
[22] C.D. Wagner, Empirical atomic sensitivity factors for quantitative analysis by electron spectroscopy for chemical analysis, Surf. Interface Anal. 3 (5) (1981) 211.
[23] J. Tetazoo, NIST x-ray photoelectron spectroscopy database, nist standard reference database 20, version 4.1, Available at, https://srdata.nist.gov/xps/.
[24] C.K. Lew, N. Dontschuk, D.A. Broadway, J.P. Tetienne, J.C. McCallum, L.C. L. Hollenberg, B.C. Johnson, Investigation of charge carrier trapping in hterminated diamond devices, Appl. Phys. Lett. 117 (2020), 143507.
[25] Y. Zhu, B. Zheng, W. Yao, L. Cao, The interface diffusion and chemical reaction between a Ti layer and a diamond substrate, Diam. Relat. Mater. 8 (1999) 1073.
[26] S. Kumaragurubaran, T. Yamada, S. Shikata, Annealing effects in H-and O-terminated P-doped diamond (111) surfaces, Diam. Relat. Mater. 17 (2008) 472.
[27] U. Rau, Oxygenation and air-annealing effects on the electronic properties of Cu(In, Ga)Se2 films and devices, J. Appl. Phys. 86 (1) (1999) 497.